

Joule heating and the thermal evolution of old neutron stars

Juan A. Miralles¹⁾, Vadim Urpin^{2,3)} and Denis Konenkov³⁾

¹⁾ Departament d'Astronomia i Astrofísica, Universitat de València,
Dr. Moliner 50, E-46100 Burjassot (Valencia), Spain

²⁾ Department of Mathematics, University of Newcastle
Newcastle upon Tyne NE1 7RU, UK

³⁾ A.F.Ioffe Institute of Physics and Technology,
194021 St.Petersburg, Russia

Abstract

We consider Joule heating caused by dissipation of the magnetic field in the neutron star crust. This mechanism may be efficient in maintaining a relatively high surface temperature in very old neutron stars. Calculations of the thermal evolution show that, at the late evolutionary stage ($t \geq 10$ Myr), the luminosity of the neutron star is approximately equal to the energy released due to the field dissipation and is practically independent of the atmosphere models. At this stage, the surface temperature can be of the order of $3 \times 10^4 - 10^5$ K. Joule heating can maintain this high temperature during extremely long time (≥ 100 Myr), comparable with the decay time of the magnetic field.

Subject headings: magnetic fields—stars: neutron—pulsars: general

Accepted for publication in The Astrophysical Journal

1 Introduction

Neutron stars are very hot at birth, with temperatures well above 10^{10} K. This heat is radiated away mainly by neutrinos from the inner layers during the first million years or so (the neutrino cooling era) and, later on, the emission of photons from the surface dominates the cooling of the star. This photon luminosity and its change with time depend on the properties of matter inside the neutron star and its magnetic field. Observations of this radiation can thus provide important information about the state of matter above and below nuclear density as well as about the magnetic field.

The magnetic field can influence the thermal evolution of neutron stars in different ways. This influence is probably less appreciable during the neutrino cooling era despite the neutrino

emissivities for some mechanisms can essentially alter in strong magnetic fields $\sim 10^{13}$. The effect of the magnetic field may be of a particular importance for neutrino processes in the inner crust where, at some conditions, the synchrotron emission may dominate the rate of neutrino cooling (Vidaurre et al. 1995).

The influence of the magnetic field on the cooling history is much more important during the photon cooling era. In the presence of a strong field ($\sim 10^{12} - 10^{13}$ G) the transport properties of plasma are different compared to those in non-magnetic neutron stars. Both the electron and radiative thermal conductivities can be affected by the field. Generally speaking, the cooling efficiency longitudinal to the field lines exceeds that in the transverse direction. This change in the thermal conductivity can have an appreciable effect on the thermal evolution (see Van Riper 1991, Nomoto and Tsuruta 1987). Besides, an anisotropic heat transport will result in a characteristic temperature difference between the hot magnetic poles of the neutron star and the relatively cold magnetic equator (see, e.g., Schaaf 1990).

Additional heating associated with the ohmic dissipation of currents may be one more important effect caused by the magnetic field. The rate of Joule heating depends on both the geometry of the magnetic field and conductive properties of plasma and may be rather high for some magnetic configurations. The total magnetic energy of the neutron star can probably reach $10^{43} - 10^{44}$ erg. Observational data on the spin and magnetic evolution of isolated pulsars provide some evidences that the field decay is rather slow in isolated pulsars. Thus, according to Narayan and Ostriker (1990) the decay time-scale is about 20 Myr. Bhattacharya et al. (1992) inferred even a longer decay time ($\geq 30 - 100$ Myr) from the same observational data. Nevertheless, even for such a slow decay the rate of Joule heating (if the decay is caused by ohmic dissipation) may be as large as $10^{28} - 10^{30}$ erg/s. Clearly, Joule heating cannot change substantially the early thermal evolution when the neutron star is relatively hot and its luminosity exceeds this value. However, the ohmic dissipation produces enough heat to change completely the thermal history of old neutron stars. Assuming that all heat released due to dissipation of the magnetic field is transferred to the surface (that is true during the photon cooling era) and emitted with the blackbody spectrum, one can obtain an estimate of the surface temperature, T_s , required to maintain the neutron star under the thermal equilibrium. This temperature may be as high as $3 \times 10^4 - 10^5$ K, and the neutron star can maintain this temperature during a long time, comparable with the decay time of the magnetic field, $\sim 30 - 100$ Myr, whereas T_s has to fall down to the value below 10^5 K after $\sim 1 - 3$ Myr in accordance with the so called standard cooling scenario. Therefore an observational and theoretical study of the late thermal evolution of neutron stars may be a powerful diagnostics of their magnetic fields and can provide an important information about the magnetic configuration and mechanisms of its decay.

Detection of the thermal radiation from old and close neutron stars with the surface temperature $\leq 10^5$ K has become possible only in recent years. Thus, Becker & Trümper (1997) detected several middle-aged and old neutron stars in the soft X-ray band. The Hubble Space Telescope also detected the optical and UV thermal emission from few relatively old pulsars (Pavlov, Stringfellow & Cordova 1996, Mignani, Caraveo & Bignami 1997). The corresponding surface temperatures turn out surprisingly high compared to predictions of the standard cooling model. Such high temperatures can be understood only if some mechanisms of additional heating operate in relatively old neutron stars.

One possible source of heating can be caused by the frictional interaction of neutron su-

perfluid with the normal matter in the inner crust (Shibazaki & Lamb 1989, Umeda et al. 1993). If the inner crust of neutron stars contains superfluid rotating faster than the rest of the star, the differential rotation causes the frictional heat generation. The authors found that the rate of a frictional heat generation does not depend on specific models for the superfluid-crust interaction. Note that the frictional heating is independent of the magnetic field whereas the Joule heating is strongly sensitive to the field strength. This difference provides a hope to discriminate between these heating mechanisms from observational data.

In the present paper, we consider the thermal evolution of a neutron star assuming the crustal origin of its magnetic field. The models with a crustal magnetic field turn out to be quite suitable to account for a wide variety of observational data on the magnetic and spin evolution of both isolated and entering binary systems neutron stars (Urpin & Kononkov 1997, Urpin, Geppert & Kononkov 1997). We calculate the rate of Joule heating caused by dissipation of currents in the neutron star crust. Incorporating the expression for Joule heating into the numerical codes of thermal evolution, we examine the effect of this heating on the cooling history. In §2 the physical model adopted for our calculations is described. The results of calculations of the thermal evolution with Joule heating are presented in §3. In §4 we briefly summaries the results of our study.

2 Basic equations

We assume that the magnetic field has been generated in the neutron star crust by some unspecified mechanism during or shortly after neutron star formation. The evolution of such a field is controlled by the conductive properties of the crust. Shortly after collapse the main fraction of the crustal material solidifies, and the evolution of the crustal field is governed by the induction equation without the convective term,

$$\frac{\partial \mathbf{B}}{\partial t} = -\frac{c^2}{4\pi} \nabla \times \left(\frac{1}{\sigma} \nabla \times \mathbf{B} \right), \quad (1)$$

where σ is the conductivity. We restrict our consideration to a dipolar field which can be described by the vector potential $\mathbf{A} = (0, 0, A_\varphi)$, $A_\varphi = S(r, t) \sin \theta / r$, where r and θ are the spherical radius and polar angle, respectively. Then the function $S(r, t)$ obeys the equation (see, e.g., Sang & Chanmugam 1987)

$$\frac{\partial^2 S}{\partial r^2} - \frac{2S}{r^2} = \frac{4\pi\sigma}{c^2} \frac{\partial S}{\partial t} \quad (2)$$

with the boundary condition

$$\frac{\partial S}{\partial r} + \frac{S}{R} = 0 \quad (3)$$

at the stellar surface $r = R$. For a field confined to the crust, $S(r, t)$ should vanish in the deep layers. The field components in the interior of the star are

$$B_r = \frac{2S}{r^2} \cos \theta, \quad B_\theta = -\frac{\sin \theta}{r} \frac{\partial S}{\partial r}. \quad (4)$$

The φ -component of the electric current maintaining the dipolar magnetic configuration is given by

$$j_\varphi = -\frac{c}{4\pi} \cdot \frac{\sin \theta}{r} \cdot \left(\frac{\partial^2 S}{\partial r^2} - \frac{2S}{r^2} \right). \quad (5)$$

Then one has for the rate of Joule heating $\dot{q} = j^2/\sigma$

$$\dot{q} = \frac{c^2}{16\pi^2\sigma} \cdot \frac{\sin^2 \theta}{r^2} \cdot \left(\frac{\partial^2 S}{\partial r^2} - \frac{2S}{r^2} \right)^2. \quad (6)$$

For the sake of simplicity, we will neglect non-sphericity in cooling calculations. Therefore, instead of equation (6), we will use the polar-averaged expression for Joule heating,

$$\dot{q} = \frac{c^2}{24\pi^2 r^2 \sigma} \left(\frac{\partial^2 S}{\partial r^2} - \frac{2S}{r^2} \right)^2. \quad (7)$$

It is convenient to normalize the function $S(r, t)$ to its initial value at the surface, $S(R, 0)$, which in its turn can be related to the initial field strength at the magnetic equator, B_e , by $S(R, 0) = R^2 B_e$. Finally, we obtain the expression for the rate of Joule heating in the form

$$\dot{q} = \frac{c^2 R^4 B_e^2}{24\pi^2 r^2 \sigma} \left(\frac{\partial^2 s}{\partial r^2} - \frac{2s}{r^2} \right)^2, \quad (8)$$

where $s(r, t) = S(r, t)/S(R, 0)$.

The evolution of the magnetic field as well as the rate of heat production is strongly sensitive to the conductivity. In the crust, the conductivity is determined by electron scattering with phonons and lattice impurities; which mechanism dominates depends on the density ρ and the temperature T . Electron-phonon scattering gives the main contribution to the conductivity at a relatively low density. For this mechanism, $\sigma \propto T^{-1}$ when T is above the Debye temperature and $\sigma \propto T^{-2}$ for lower T . Electron-impurity scattering becomes more important with increasing density and decreasing T . When it dominates, σ is nearly independent of T , and its magnitude depends on the impurity parameter

$$\xi = \frac{1}{n_i} \sum_{n_\alpha} n_\alpha (Z - Z_\alpha)^2,$$

where n_i and Z are the number density and charge number of the dominant background ion specie, respectively, and n_α is the number density of an interloper specie of charge Z_α ; the summation is over all species of impurities. In our calculations, we use the numerical data on the phonon conductivity obtained by Itoh et al. (1993) and the analytical expression for the impurity conductivity derived by Yakovlev & Urpin (1980).

Our cooling calculations taking into account the additional heating caused by the ohmic dissipation have been done within the *isothermal approximation* that follows from assuming constant temperature (corrected by the redshift factor) in the interior of the star ($\rho > 10^{10}$ g/cm³) and a temperature drop at the surface given by the atmosphere model that relates the interior temperature with the effective temperature (outer boundary condition) and allows to calculate the photon luminosity of the star. Although the calculations presented here correspond

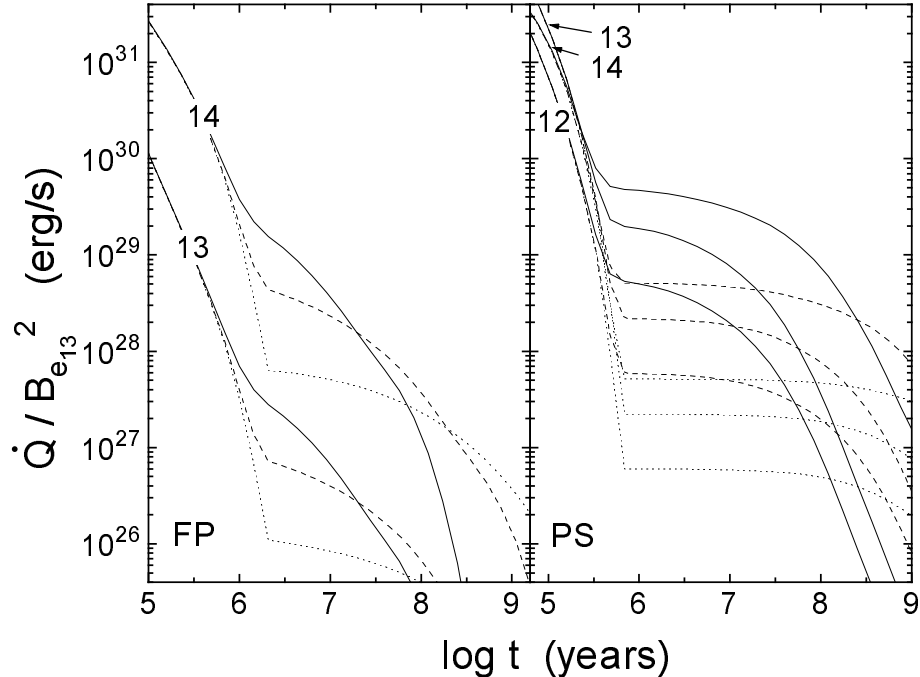


Figure 1: The time dependence of the rate of Joule heating integrated over the star volume and normalized to $B_{e13} = B_e/10^{13}$ G. Numbers near the curves indicate the logarithm of ρ_0 . Different types of lines correspond to different values of ξ : 0.1 (solid), 0.01 (dashed), 0.001 (dotted).

to the isothermal approximation we have checked for isothermality running some models where this restriction is not enforced. At time when Joule heating becomes important, the thermal conductivity of the crust is so high that the isothermal condition is very well satisfied and we do not observe significant differences in the thermal evolution with respect to the isothermal approximation.

We use the atmosphere models calculated by Van Riper (1988) to impose the outer boundary condition to the cooling calculations. These atmosphere models are obtained by solving the hydrostatic and radiative equilibrium equations for a pure ^{56}Fe composition (see Van Riper 1988 for details).

Calculations presented here are based on the so called *standard cooling scenarios* which correspond to a star with standard neutrino emissivities. We consider the thermal history for $1.4M_\odot$ models constructed with the equations of state of Friedman and Pandharipande (1981; hereafter FP) and Pandharipande and Smith (1976; hereafter PS). The PS model is representative of stiff equations of state with a low central density and a massive crust; the FP model represents intermediate equations of state. The stiffer the equation of state, the larger the radius and crustal thickness for a given neutron star mass. For the FP and PS models, the radii are 10.61 km and 15.98 km, respectively; the corresponding crustal thicknesses are ≈ 980 m and 4200 m; the crust bottom is located at the density 2×10^{14} g/cm 3 . Our choice is imposed by the fact that only models with the equation of state stiffer than that of Friedman and Pandharipande seem to be suitable to account for the available observational data on the magnetic evolution of pulsars (Urpin & Konenkov 1997).

3 Numerical results

In our calculations, we assume the initial magnetic field to be confined to the outer layers of the crust with density $\rho \leq \rho_0$. The calculations have been performed for a wide range of ρ_0 , $10^{14} \geq \rho_0 \geq 10^{12}$ g/cm³. In the present paper, we choose the initial function $s(r, 0)$ in the form

$$s(r, 0) = (1 - r^2/r_0^2)/(1 - R^2/r_0^2), \quad r \geq r_0$$

$$s(r, 0) = 0, \quad r < r_0$$

where r_0 is the boundary radius of the region originally occupied by the magnetic field, $\rho_0 = \rho(r_0)$. Note that the field decay and Joule heating are sensitive to the initial depth penetrated by the field and, hence, to the value ρ_0 . However, both these quantities are much less affected by the particular form of the original field distribution.

The impurity parameter, ξ , is taken within the range $0.1 \geq \xi \geq 0.001$ and it is assumed to be constant throughout the crust. This parameter plays a key role in any model of the magnetic evolution of neutron stars but, unfortunately, there are no reliable theoretical estimates of ξ . Calculations of the impurity charge and concentration in the crust meet troubles because of large uncertainties in the non-equilibrium processes during the very early evolution of a neutron star. Flowers & Ruderman (1977) made an attempt to estimate the final crustal composition taking into account slow neutrino reactions at $T < 10^{10}$ K (but above the melting point). They calculated small deviations from the equilibrium composition predicted by energy-minimisation criteria and estimated $\xi \approx 0.004$. However, this estimate contains the binding energies of nuclei in the exponential factor thus the obtained value is rather uncertain. The properties of the crust can also be influenced by accretion during the early phase after the supernova explosion (see, e.g, Chevalier 1989). During this phase, the unbind fraction of matter falls back onto the neutron star surface and the total amount of accreted mass may be as large as $0.1M_\odot$. Evidently, this material can substantially change the crustal composition and increase the impurity parameter. Besides, ξ can generally be non-uniform within the crust (De Blasio 1998) because mixing between the layers with different composition may be an important mechanism of the impurity production. Note also that calculations of the magnetic evolution of neutron stars with the crustal magnetic field (Urpin & Kononkov 1997) give a better fit to observational data if $\xi \sim 0.1 - 0.01$.

Figure 1 plots the evolution of the rate of Joule heating integrated over the neutron star volume,

$$\dot{Q} = 4\pi \int_0^R \dot{q}r^2 dr ,$$

for the FP and PS models. Calculations have been performed for few values of ρ_0 and ξ . At $t > 1$ Myr, the efficiency of Joule heating at given ρ_0 turns out to be essentially different for the FP and PS models with a much lower rate of heating for the FP model. This difference is evident because the thickness of the crust is much smaller for the FP model and, hence, the field strength decreases faster. Since the rate of Joule heating is proportional to j_φ^2 , it is much greater during the late evolution for the PS model which experiences a lower field decay. The rate of heating is very sensitive to the initial depth penetrated by the field. If the field is initially confined to the layers with density $\rho < 10^{14}$ g/cm³ for the FP model and $\rho < 10^{12}$ g/cm³ for the PS model then, after ~ 1 Myr, the rate of heating is likely too low to heat the

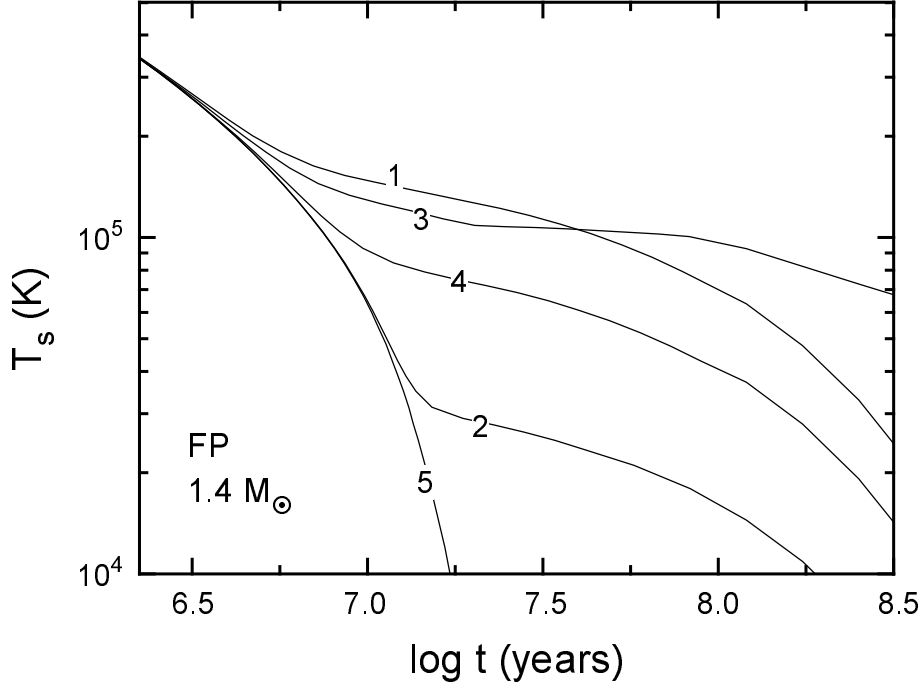


Figure 2: The thermal evolution of the FP model with and without Joule heating; curve 1 – $B_e = 1.5 \times 10^{13}$ G, $\rho_0 = 10^{14}$ g/cm³, $\xi = 0.1$; curve 2 – $B_e = 1.5 \times 10^{13}$ G, $\rho_0 = 10^{13}$ g/cm³, $\xi = 0.1$; curve 3 – $B_e = 1.5 \times 10^{13}$ G, $\rho_0 = 10^{14}$ g/cm³, $\xi = 0.01$; curve 4 – $B_e = 5 \times 10^{12}$ G, $\rho_0 = 10^{14}$ g/cm³, $\xi = 0.1$; curve 5 – without Joule heating.

neutron star to a sufficiently high surface temperature even if the initial magnetic field is of the order of the maximal field observed in neutron stars, $\sim 4 \times 10^{13}$ G. Note that, at $t < 1$ Myr, the effect of Joule heating on the thermal evolution is negligible (see below). The rate of heating is also sensitive to the impurity parameter ξ . For a given ρ_0 and B_e , \dot{Q} is initially higher for larger values of ξ since the conductivity is lower for such ξ . However, a lower conductivity leads to a faster decrease of the field strength and, hence, \dot{Q} . At some age (which generally depends on ρ_0 and ξ), the heat production becomes larger for a smaller ξ . Note that the ohmic dissipation can maintain the rate of heating at approximately the same level during extremely long time. Thus, for a very pure crust with $\xi = 0.001$, the neutron star may have a practically constant surface temperature during ≈ 1000 Myr after the initial cooling stage ($t < 1 - 3$ Myr). For more polluted crust with $\xi = 0.01$, this phase of almost constant surface temperature can last ~ 100 Myr.

Figure 2 shows the thermal evolution of the neutron star with Joule heating and with the FP equation of state. We plot the cooling curves only for the age $t > 2 \times 10^6$ yr since the earlier evolution is not affected practically by Joule heating. For a comparison, the cooling history of a non-magnetized neutron star is also shown. All the cooling curves presented in this paper are obtained considering a non-magnetized atmosphere. This is done so for the sake of simplicity in the comparison of the different models. Had we used magnetic atmospheres we would have obtained significant differences in the evolution of the surface temperature with respect to the non-magnetized atmospheres only before the Joule heating drives the evolution but not after this time, as we will explain bellow.

It turns out that Joule heating may have an appreciable influence on the thermal evolution of the FP model only if the magnetic field occupies initially a significant fraction of the crust volume and if the field is initially very strong. Therefore, calculations presented here have been performed for $B_e \geq 5 \times 10^{12}$ G and $\rho_0 = 10^{13}$ and 10^{14} g/cm³. Note that the value $\rho_0 = 10^{14}$ g/cm³ corresponds to a depth from the surface of ≈ 660 m, thus, about 60% of the crust volume has to be occupied initially by the field. Except a short initial phase ($\sim 3 - 10$ Myr) when the surface temperature is high, the effect of Joule heating on neutron star cooling turns out surprisingly simple: approximately all heat released due to the field dissipation has to be emitted from the surface, thus, the surface temperature T_s obeys with a high accuracy the equation

$$\dot{Q} \approx 4\pi R^2 \sigma_{SB} T_s^4, \quad (9)$$

where σ_{SB} is the Stephan-Boltzmann constant. The heat flux to the interior is negligible for all considered models and, therefore, the luminosity of old neutron stars has to be completely determined by the field strength and geometry and the conductive properties of the crust. Note that equation (9) is also valid for the PS model (see below).

If the initial field of a neutron star is of the order of the maximal pulsar field, $B_e \sim (3-4) \times 10^{13}$ G, Joule heating can maintain a relatively high surface temperature $\sim 5 \times 10^4 - 10^5$ K in relatively old neutron stars with $t \geq 10$ Myr. Evidently, this temperature is much above the surface temperature predicted by the standard cooling models without additional heating mechanisms. For the FP model, the neutron star can stay in such a “warm” state rather long, $\sim 30 - 60$ Myr. The efficiency of heating is very sensitive to ρ_0 : if the field is initially anchored in the layers with $\rho \leq 10^{13}$ g/cm³ the surface temperature at $t > 10$ Myr turns out to be lower than 3×10^4 K even for the maximal pulsar field.

In Figure 3, we plot the thermal evolution of the PS model with and without Joule heating. The cooling curves are shown only for $t > 2$ Myr since for the earlier age the influence of Joule heating is unimportant. Like in the case of the FP model, at the late evolutionary stage ($t > 10$ Myr) the surface temperature of the PS model is determined by balancing the Joule heating with the photon luminosity (equation 9). However, for the PS model the effect of additional heating is much more pronounced because the field decay is substantially slower and, after 10 Myr of evolution, the field is stronger for this model. The surface temperature caused by Joule heating may be as high as $3 \times 10^4 - 10^5$ K even if the field occupied initially a relatively small fraction of the crust volume. It turns out that T_s is strongly sensitive to all parameters determining the magnetic evolution (ξ , ρ_0 , B_e). At $t > 10$ Myr, a relatively high temperature ($T_s \geq 5 \times 10^4$ K) can be reached only for strongly magnetized neutron stars with the initial field $B_e \geq 5 \times 10^{12}$ G. The surface temperature is rather low if the magnetic field is initially confined to the layers with a small density, $\rho \leq 10^{12}$ g/cm³. This is due to the fact that the crustal field anchored initially in not very deep layers experiences a fast decay during the very early evolutionary stage ($t < 10^5$ yr) when the neutron star is hot and the crustal conductivity is low. For such initial magnetic configurations, the field strength at $t > 10$ Myr is too weak to produce an appreciable Joule heating. The most remarkable point is that all considered models with Joule heating can maintain a sufficiently high temperature during extremely long time. Thus, our calculations show that for the “polluted” crust ($\xi = 0.1$) T_s decreases only by a factor ~ 3 when t runs from 10 to 100 Myr. For $\xi = 0.01$, the temperature is practically unchanged during the same period. Evidently (see equation 9), the characteristic cooling time in our model is determined by the ohmic decay time of the magnetic field and, therefore, should

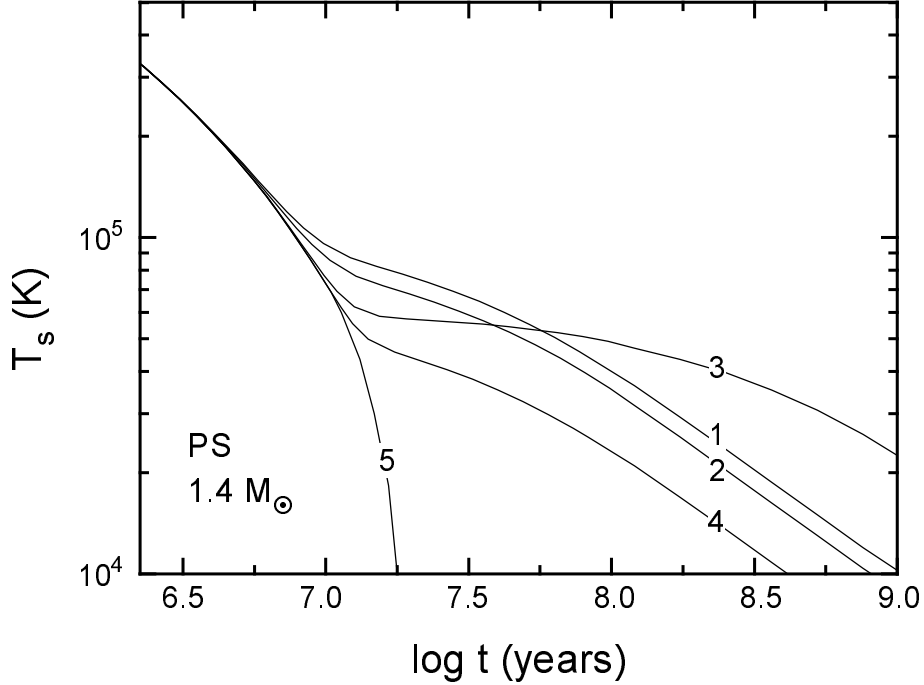


Figure 3: The thermal evolution of the PS model with and without Joule heating; curve 1 – $B_e = 1.5 \times 10^{13}$ G, $\rho_0 = 10^{13}$ g/cm³, $\xi = 0.1$; curve 2 – $B_e = 1.5 \times 10^{13}$ G, $\rho_0 = 5 \times 10^{12}$ g/cm³, $\xi = 0.1$; curve 3 – $B_e = 1.5 \times 10^{13}$ G, $\rho_0 = 10^{13}$ g/cm³, $\xi = 0.01$; curve 4 – $B_e = 5 \times 10^{12}$ G, $\rho_0 = 10^{13}$ g/cm³, $\xi = 0.1$; curve 5 – without Joule heating.

be very long.

Note that a simple estimate of the surface temperature caused by Joule heating can be obtained directly from equation (9). The rate of heat production is equal to the rate of decrease of the magnetic energy. In the main fraction of the crust volume (except surface layers and a region near the magnetic pole), θ -component of the crustal field is stronger than the radial one, which in its turn is of the order of the current surface field, $B(t)$. We have $B_\theta \sim B_r(R/\ell) \sim B(t)(R/\ell)$ (see equation (4)) where ℓ is the radial lengthscale of the magnetic field; this lengthscale depends on time since the field diffuses inwards. Therefore, the energy of the crustal field can be estimated as $E_m \sim 4\pi R^2 \ell (B_\theta^2/8\pi)$ and, correspondingly, $\dot{Q} \sim E_m/t$. Substituting this expression into equation (9), we obtain the estimate of the surface temperature,

$$T_s \sim \left(\frac{R^2 B^2(t)}{8\pi \sigma_{SB} \ell t} \right)^{1/4},$$

or

$$T_s \sim 4 \times 10^4 B_{12}^{1/2}(t) R_6^{1/2} \ell_5^{-1/4} t_8^{-1/4} \text{K}, \quad (10)$$

where $B_{12}(t) = B(t)/10^{12}$ G, $R_6 = R/10^6$ cm, $\ell_5 = \ell/10^5$ cm, and $t_8 = t/10^8$ yr. In this equation, both the current field strength, $B(t)$, and the depth penetrated by the field, ℓ , depend generally on the impurity parameter, ξ , and these dependences are rather complex because of a non-uniform chemical composition of the crust. Nevertheless, sometimes, the estimate (10) may be useful because the dependence of T_s on ℓ is weak, and ℓ varies within a relatively narrow range.

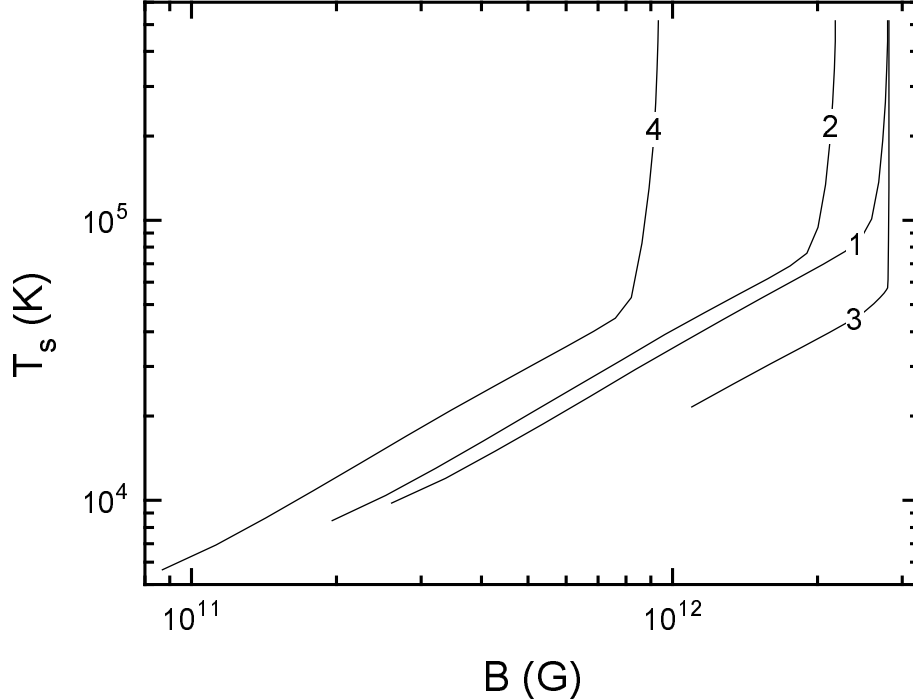


Figure 4: The dependence of the surface temperature, T_s , on the current equatorial magnetic field, B , for the PS model. Numbers near the curves correspond to the same values of parameters as in Fig.3.

For example, for the models presented here, ℓ_5 is ranged from 0.5 to 1 for the FP model and from 1 to 4 for the PS model. Of course, this simplified estimation is only valid soon after the Joule heating becomes important $t \sim 10\text{--}30$ Myr till the magnetic field reaches the crust–core boundary ($t \sim 1000$ Myr for the PS model).

Obviously, in the suggested mechanism, the rate of Joule heating and the surface temperature depend strongly on the current magnetic field strength at the equator, B . In Figure 4, we plot the dependence of the surface temperature on B for the PS neutron star model. The chosen range of the field strength corresponds to the age from ~ 3 Myr to ~ 1000 Myr (see Fig.3). Note that the magnetic field strength, plotted in Fig.4, is different from what is usually calculated using observational data on the pulsar period, P , and its derivative, \dot{P} , and assuming magnetodipole braking. The standard estimate (Ostriker & Gunn 1969) gives the field strength at the magnetic equator,

$$B_{obs} = (3Ic^3 P \dot{P} / 8\pi^2 R^6)^{1/2}, \quad (11)$$

where I is the moment of inertia. However, this equation gives an estimate of the equatorial field produced by the component of the magnetic dipole perpendicular to the spin axis because the parallel component does not contribute to braking. The rate of Joule heating is determined by the true magnetic field produced by the both components. Therefore, the equatorial field strength entering our calculations is by a factor $1/\sin \alpha$ larger than the observable pulsar magnetic field, B_{obs} , where α is the angle between magnetic and spin axes.

To plot $T_s(B)$, we simply eliminate the t -dependence from the cooling curves, $T_s(t)$, and the magnetic decay curves, $B(t)$, calculated for the same values of initial parameters (for

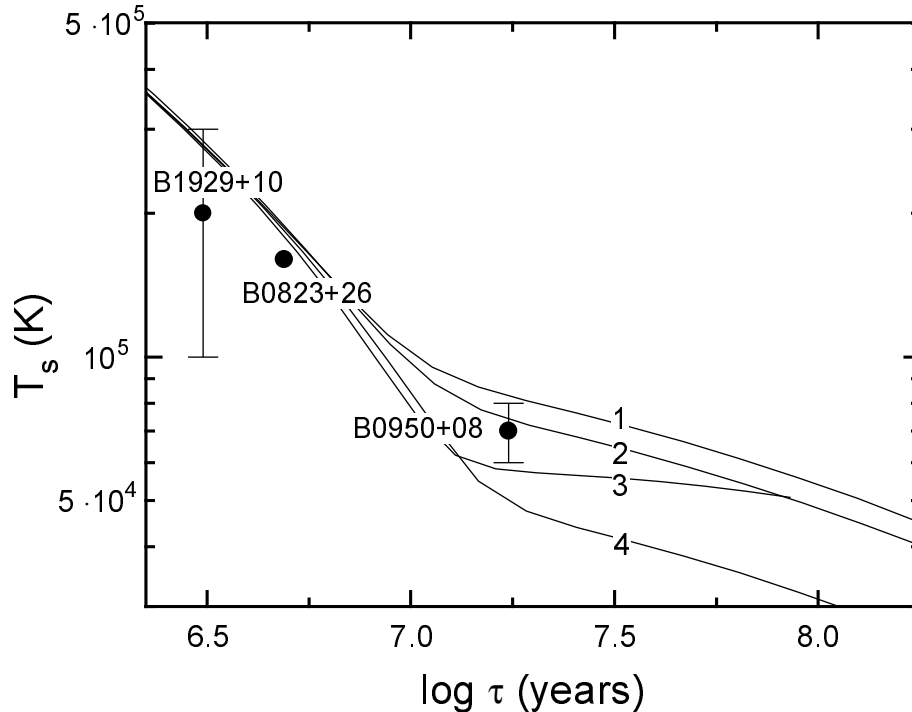


Figure 5: The dependence of the surface temperature, T_s , on the spin-down age, τ , for the PS model. Numbers near the curves correspond the same values of parameters as in Fig.3.

more details concerning magnetic decay curves see Urpin & Konenkov 1997). Obviously, T_s decreases with the magnetic field decay. During the first several Myr while Joule heating is negligible, the magnetic evolution is going much slower than the thermal one because neutrino emissivity and photon luminosity make the characteristic cooling time much shorter than the characteristic time for ohmic decay. This phase of evolution (represented by nearly vertical pieces of curves) lasts while the total rate of Joule heating, \dot{Q} , is smaller than the luminosity. At $B \leq (1 - 3) \times 10^{12}$ G (depending on the parameters) when Joule heating plays a dominating role in the thermal evolution, the characteristic cooling time becomes comparable with the decay time of the magnetic field as it follows from equation (9).

Figure 5 shows the dependence of the surface temperature on the spin-down age of neutron stars with the PS equation of state. Our knowledge of the field strength and its behaviour with time comes mainly from radio pulsars with measured spin-down rates. For the most of pulsars, the true age is unknown and observations provide information only on the so called spin-down age, $\tau = P/2\dot{P}$. Therefore, for a comparison with observational data, it is convenient to analyse the dependence of T_s on τ rather than on t . Assuming magnetodipole braking and integrating equation (11), we can calculate the spin-down age as a function of time, $\tau = \tau(t)$. Eliminating t from the couple of functions $T_s(t)$ and $\tau(t)$, we obtain the dependences $T_s(\tau)$ shown in Figure 5.

The τ -dependence of cooling curves is qualitatively similar to their t -dependence. The only difference is a bit slower decrease of T_s in terms of the spin-down age. This difference is clear because $\tau(t) > t$ for a decaying magnetic field. In Figure 5, we also plot the data for three middle age and old pulsars: B0823+26 ($\tau = 4.9$ Myr), B1929+10 ($\tau = 3$ Myr) and B0950+08

($\tau = 17.4$ Myr). The surface temperatures of these pulsars are $\sim 1.6 \times 10^5$ (this estimate has been obtained from the luminosity given by Becker & Trümper, 1997, assuming the black-body spectrum), $(1 - 3) \times 10^5$ and $(7 \pm 1) \times 10^4$ K (Pavlov, Stringfellow & Cordova 1996), respectively. Of course, these observational data are too poor to infer somewhat categorical but, nevertheless, it seems that the ohmic dissipation can produce enough heat to maintain the observed surface temperatures of middle age and old pulsars.

4 Summary

We considered Joule heating caused by the decay of the crustal magnetic field in neutron stars. Calculations of the thermal evolution of neutron stars show that the heat released in the crust due to the field decay diffuses mainly outward thus practically all the Joule heat has to be radiated from the surface. Due to this, the surface temperature at the late evolutionary stage ($t > 10$ Myr) turns out to be independent of the atmosphere models and is determined by balancing between the rate of Joule heating integrated over the neutron star volume and the luminosity (see equation (9)). Being independent of the atmosphere models, T_s is however strongly dependent on parameters of the magnetic configuration and the conductive properties of the crust. Therefore, the observational study of the late thermal history of neutron stars could be a useful diagnostic of their internal magnetic fields and properties of the crust.

The decay of the crustal magnetic field can produce enough heat to maintain a sufficiently high surface temperature $\sim 3 \times 10^4 - 10^5$ K. Our calculations predict that Joule heating becomes important after a relatively short ($\sim 3 - 10$ Myr depending on the model) initial phase when the neutron star cools down to $T_s \sim 3 \times 10^4 - 10^5$ K. The further thermal evolution slows down substantially: a characteristic cooling time becomes comparable with the decay time of the magnetic field. Since the field decay in the crust is very slow, the neutron star can maintain a surface temperature practically unchanged during extremely long time, $t \geq 100$ Myr.

Acknowledgement

This work has been supported in part by the Spanish DGICYT (grant PB94-0973) and by the Russian Foundation of Basic Research (grant 97-02-18086). It is a pleasure to thank Ken Van Riper for useful discussions.

References

- Becker, W., & Trümper, J. 1998, A&A (in press)
- Bhattacharya, D., Wijers, R., Hartman, J., & Verbunt, F. 1992, A&A, 254, 198
- Chevalier, R. 1989, ApJ, 346, 847
- De Blasio, F. 1998, MNRAS (in press)
- Flowers, E., Ruderman, M. 1977, ApJ, 215, 302
- Friedman, B., Pandharipande, V.P. 1981, Nucl.Phys. A, 361, 502
- Itoh, N., Hayashi, H., Kohyama, Y. 1993, ApJ, 418, 405
- Mignani, R., Caraveo, P.A., & Bignami, G. 1997, ApJ, 474, L51
- Narayan, R., & Ostriker, J.P. 1990, ApJ, 352, 222
- Nomoto, K., & Tsuruta, S. 1987, ApJ, 312, 711
- Ostriker, J.P., & Gunn, J.E. 1969, ApJ, 157, 1395
- Pandharipande, V.R., Pines, D., Smith, R.A. 1976, ApJ, 208, 550
- Pavlov, G., Stringfellow, G.S., & Cordova, F.A. 1996, ApJ, 467, 370
- Sang, Y., & Channugam, G. 1987, ApJ, 323, L61
- Schaaf, M.E. 1990, A&A, 227, 61
- Shibazaki, N., & Lamb, D. 1989, ApJ, 346, 808
- Umeda, H., Shibazaki, N., Nomoto, K., & Tsuruta, S. 1993, ApJ, 408, 186
- Urpin, V., & Konenkov, D. 1997, MNRAS, 292, 167
- Urpin, V., Geppert, U., & Konenkov, D. 1998, MNRAS (in press)
- Van Riper, K. 1988, ApJ, 329, 339
- Van Riper, K. 1991, ApJS, 75, 449
- Vidaurre, A., Pérez, A., Sivak, H., Bernabéu, J., & Ibáñez, J.M. 1995, ApJ, 448, 264
- Yakovlev, D., & Urpin, V. 1980, SvA, 24, 303